High-performance Surface-normal Modulators Based on Stepped Quantum Wells

H. Mohseni
Department of Electrical and Computer Engineering, Northwestern University
Evanston, IL 60208; e-mail: hmohseni@ece.northwestern.edu

W. K. Chan, H. An, A. Ulmer, and D. Capewell
Sarnoff Corporation, 201 Washington Road, Princeton NJ 08543

Abstract: We present high-performance surface-normal modulators based on unique properties of stepped quantum wells (SQWs) around the eye-safe wavelength of 1550 nm. Fabricated devices show nearly two times better efficiency and 7 dB higher extinction ratio compared with the conventional devices with rectangular and coupled-quantum well active layers. Moreover, the optical bandwidth is about 70 nm at a 3dB modulation depth, which is more than five times wider than the optical bandwidth of the conventional devices. Such a wide optical bandwidth eliminates the need for a temperature controller. This is a critical advantage for many applications such as unmanned aerial vehicles (UAVs) and dynamic optical tags (DOTs), where limited volume, power, and weight can be allocated to the modulator system.

I. Introduction

Surface-normal optical modulators are attractive devices for applications in free-space photonic link between mobile platforms[1] as well as for optical interconnects[2]. Although several surface-normal modulator technologies are available, p-i-n quantum well based modulators are the most attractive of these because they operate at the highest frequency and over the widest temperature range. Nevertheless, these devices still suffer from high power consumption, limited data bandwidth, and limited optical bandwidth. Reducing the device area can directly improve the power consumption and data bandwidth, since the former is inversely and the latter is directly proportional to the device area. Unfortunately, reducing the device area can significantly degrade the link performance, since the gain of a photonic link based on a retroreflector is proportional to the fourth power of the modulator area[1]. Recently, coupled quantum wells have been used to reduce the operating voltage, and hence the power consumption, of the modulator[3]. However, the data bandwidth of these devices is still limited by RC to about 15 MHz, and the optical bandwidth is only about 10 nm. Low optical bandwidth is particularly unfavorable, since the change of modulator temperature can change the modulator bandgap and hence reduce the modulation depth significantly. Consequently, a low optical bandwidth leads to significantly higher system power consumption, cost, and volume due to the need for temperature control.

Enabling Photonics Technologies for Defense, Security, and Aerospace Applications,
edited by A. R. Pirich, M. J. Hayduk, E. J. Donkor, P. J. Delfyett, Jr., Proc. of SPIE Vol. 5814
(SPIE, Bellingham, WA, 2005) · 0277-786X/05/$15 · doi: 10.1117/12.607320

Here we report on realization of a large area surface-normal modulator based on stepped quantum wells[4,5] with very low capacitance per unit area, wide optical bandwidth, wide field of view, high extinction ratio, and high efficiency.

II. Modeling

We developed a modeling and simulation software package for semiconductor-based optical modulators. Figure 1 shows the software interface with calculated electron, heavy, and light-hole wavefunctions for a given set of material composition and thickness. The optical absorption spectrum of the quantum well was then calculated using an effective mass approach. The excitonic effect was calculated based on a variational method[6]. The electric field inside the active region was calculated using diffusion-drift and Poisson equations.

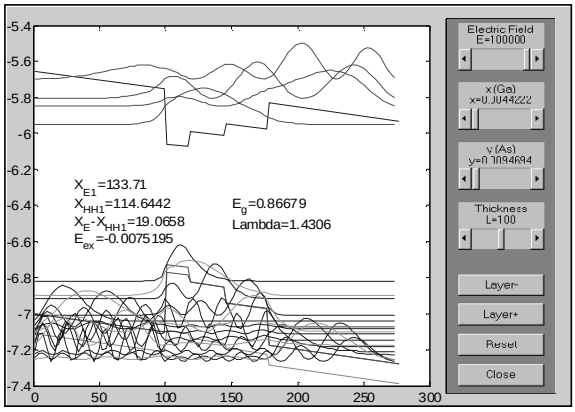

Figure 1. A snapshot of the simulation software.

Optical absorption coefficient versus the applied bias to the device (see Figure 2) was calculated from the electric field and applied voltage relationship, combined with the optical absorption and applied field relationship.

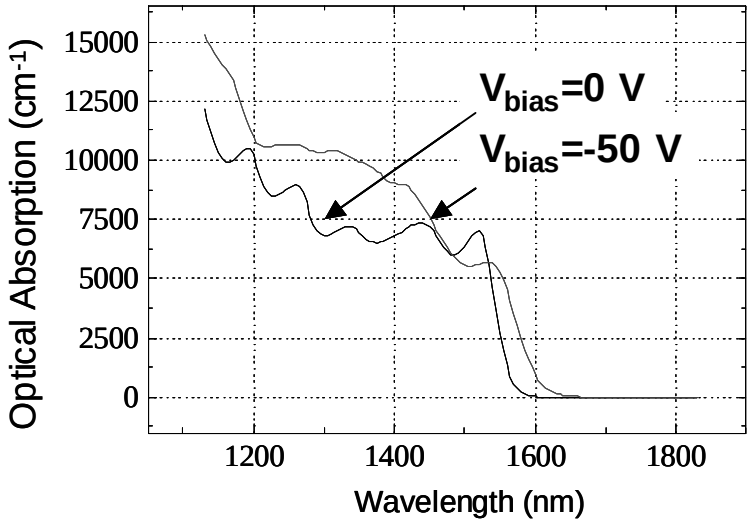

Figure 2. Calculated optical absorption coefficient versus applied bias for the device.

III. Modulator Implementation

Modulator structure is based on GaInAsP/AlInAs material grown by low-pressure metal organic vapor phase epitaxy (MOVPE) on n-type InP substrates. The active layer contains 248 periods of stepped quantum wells with a total thickness of about 5 μm, and is sandwiched between the n-doped InP and a 1 μm thick p-doped AlInAs layer. All layers are nominally lattice matched to the InP substrate to reduce defect related current leakage current, and improve the yield. The material is processed into mesa-type modulators with different diameters from 250 μm to 6.3 mm (Figure 3).

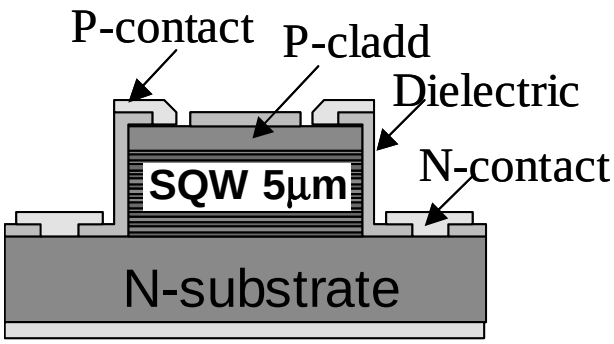

Figure 3. Schematic of the processed device.

IV. Measurement and Results

High leakage current and premature breakdown are the most important source of low yield for large area modulators. We used a dielectric based passivation method to reduce the surface leakage current (see Figure 3). Figure 4 shows excellent current-voltage characteristics of a modulator with 5.1 mm diameter at zero illumination at room temperature. The dark current of the device is ~10 μA at –95 volts, which is equal to a current density of ~50 $\mu A/cm^2$ at an electric field of ~190kV/cm. This is similar to the lowest leakage current density of modulators based on InGaAs/GaAs multi-quantum wells with a much wider bandgap and at a similar electric field[7]. Also, the device shows a current that is proportional to the square root of voltage up to -80 volts. Therefore, the leakage is generation-recombination limited up to a very high voltage at room temperature.

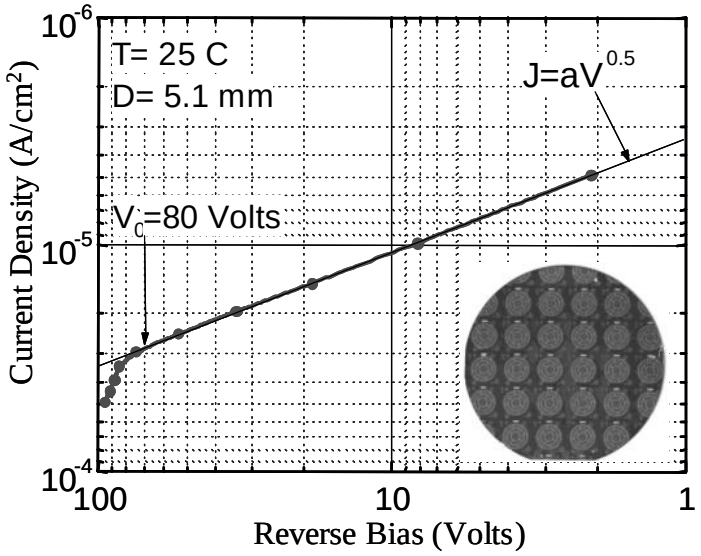

Figure 4. Current-voltage characteristic of a 5.1 mm modulator. Inset shows a fully processed 2-inch wafer.

We measured the optical transmission of the modulators using a tunable laser, a broad-area InGaAs detector, and a lock-in amplifier as detailed in Figure 5.

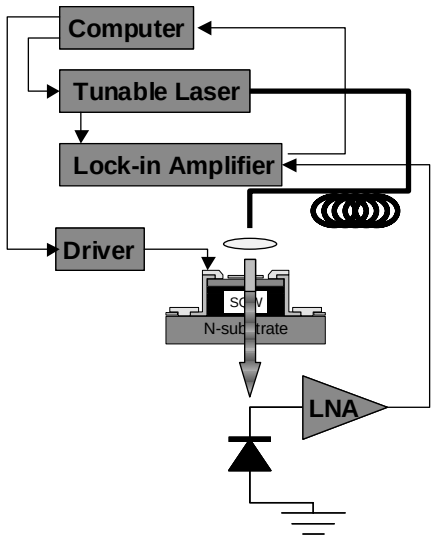

Figure 5. Normal-incident transmission measurement setup.

Fig 2-b shows the double-pass extinction ratio of a 5.1 mm device at different bias values. The extinction is more than 3 dB for 10 volts, which is similar to the extinction ratio of coupled-quantum well devices at 6 volts [2].

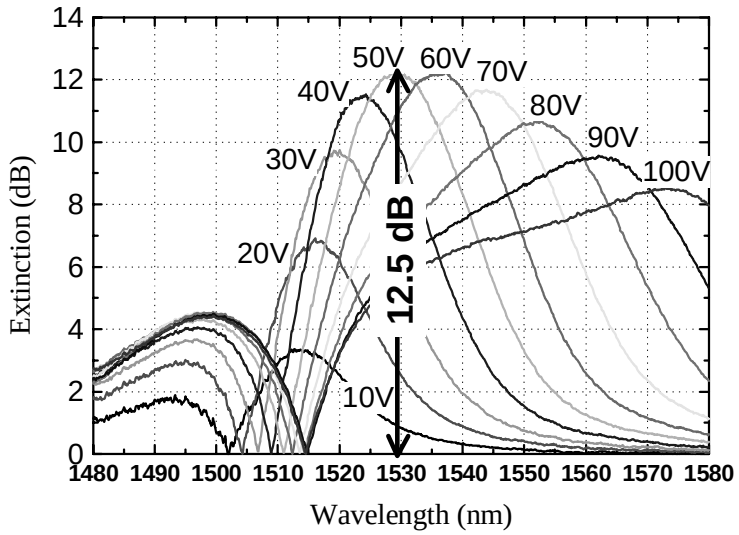

Figure 6. Measured double-pass extinction ratio spectra versus bias voltages from 0 to 100 volts.

However, the thickness of this device is five times larger, and hence the capacitance is five times smaller. Since power consumption of a modulator at high frequencies is proportional to CV^2, where C is the device capacitance and V is the applied voltage, current device consumes almost half the power of coupled-quantum well devices. Also, the maximum extinction ratio of the modulator exceeds 12 dB, which is similar to the best-reported value for devices with an internal cavity. The absence of an internal cavity in this device however, provides an extremely wide field of view that is crucial for mobile platform applications. In fact, this device has an improved extinction for beams coming at an angle, since their path-length is increased by ~$(1\text{-}0.1\sin(\theta)^2)^{-1/2}$, where θ is the angle from normal.

More importantly, the optical bandwidth of the modulator is more than 60 nm for an extinction of 3 dB and signal level of 80 volts. Change of absorption edge versus temperature in this material is nearly 0.6 nm/°C, and hence applying a signal level of 80 volts ensures that the modulator has extinction above 3 dB over a 100°C range (see Figure 6).

Although a high extinction ratio is crucial for analog applications, digital applications only require a moderate extinction around 3 dB. The signal to noise ratio of a digital free-space link can be calculated from[8]:

$$SNR = \frac{\left(\beta_{\det} \cdot P_r\right)^2}{2eFBG\left(\beta_{\det}\left(P_r + P_b\right) + i_{\det}\right) + \dfrac{2kTB}{R_L}} \quad \textbf{Eq.1}$$

where:

$\beta_{\text{det}} = G \cdot \beta$ = Detector responsivity [A/W]
G = Detector (APD/PMT) gain
$\beta = \frac{e\eta\lambda}{hc}$ = Photoemitter responsivity [A/W]
e = Charge of electron [Coul]
η = Photoemitter quantum efficiency
P_r = Received optical signal power [W]
P_b = Background illumination power [W]
F = Detector (APD/PMT) excess noise factor
B = System electrical bandwidth [Hz]
$i_{\text{det}} = G \cdot i_{dark}$ = Detector dark current [A]
i_{dark} = Photoemitter dark current [A]
k = Boltzmann's constant [J/K]
T = System noise temperature [K]
R_L = Load resistance [Ω]

The received optical power P_r is related to the modulation depth α_R :

$$P_r \propto \frac{4\alpha_R}{(1+\alpha_R)^2}; \quad \alpha_R = 1 - 10^{-\frac{ER}{10}} \qquad \textbf{Eq. 2}$$

Where *ER* is the extinction ratio in dB. Using Eq.2, one can show that an extinction ratio of 3 dB reduces *SNR* only to 89% of its maximum value. Since the power consumption increases with extinction ratio, it is logical to limit the extinction ratio to 2 to 3 dB for digital applications. We applied a signal level of 10 volts in addition to an adjustable DC bias.

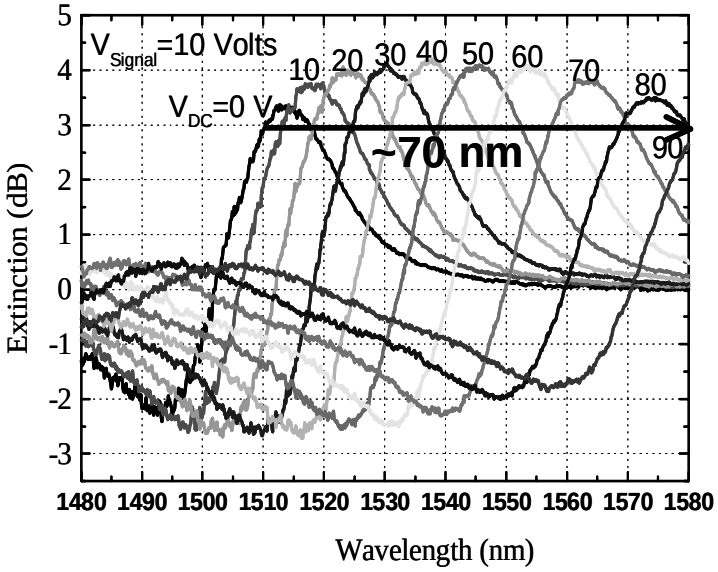

Figure 7. Measured double-pass extinction ratio spectra for a signal level of 10 volts and DC bias voltages from 0 to 90 volts.

The signal level is enough to produce an extinction ratio between 3.5 and 4.2 dB over the entire wavelength range, while a DC bias up to 90 volts could shift the peak modulation wavelength by about 70 nm (see Figure 7).

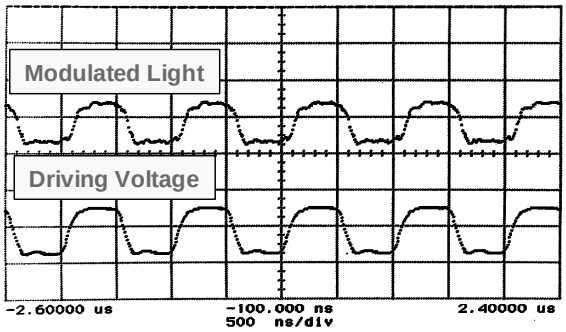

Figure 8. Single pass modulated optical signal for a 1 MHz square wave input signal.

The frequency response of the device was measured with a high voltage amplifier, and a fast infrared detector. Figure 8 shows the modulated optical signal for a square wave input signal at 1 MHz at λ~1550 nm. The large-signal performance is limited by the maximum current of the driver to about 200 nsec rise and fall times. However, small-signal 3 dB frequency bandwidth of the device exceeds 10 MHz.

VI. Conclusion and Future Work

We have successfully modeled, fabricated, and tested large-area surface-normal modulators based on stepped quantum wells. These devices show more than 12 dB extinction ratio, and nearly 70 nm tunable range. They consume almost half the power of the coupled-quantum well devices at a similar extinction ratio and data rate. More importantly, these devices can compensate thermal bandedge shift over 100°C with only 900 μW maximum power consumption. This power is two orders of magnitude less than the power required by the best thermoelectric (TE) coolers to keep the temperature of the device stable over this range.

We believe that the performance of these devices can be significantly improved with better quantum well designs, better material growth, and better device processing. In particular, we limited our optimization to a class of novel quantum wells, namely three-stepped quantum wells. Also the device leakage is generation-recombination limited, and not diffusion limited. Finally, the yield of large area devices is still quite low.

VI. Acknowledgment

Authors would like to acknowledge the partial support of DARPA ATO's Dynamic Optical Tags (DOTs) program.

VI. References

[1] G. C. Gilbreath, et.al., "Large Aperture Multiple Quantum Well Modulating Retroreflector for Free Space Optical Data Transfer on Unmanned Aerial Vehicles", Opt.Eng., **40** (7), pp. 1348-1356 (2001).

[2] H. Liu, C. C. Lin, and J. S. Harris, "High-speed, dual-function vertical cavity multiple quantum well modulators and photodetectors for optical interconnects," Opt. Eng. 40, 1186–1191 (2001).

[3] T. H. Stievater, W. S. Rabinovich, Peter G. Goetz, R. Mahon, and S. C. Binari, "A Surface-Normal Coupled-Quantum-Well Modulator at 1.55 Microns," IEEE Proceeding Conference on Lasers and Electro-optics CLEO'04, CThH3, San Francisco, California, May 2004.

[4] H. Mohseni, H. An, Z. Shellenbarger, M. Kwakernaak, and J. Abeles, "Enhanced electro-optic effect in GaInAsP–InP three-step quantum wells," Appl. Phys. Lett. **84** (11), pp. 1823-1825 (2004).

[5] H. Mohseni, H. An, Z. Shellenbarger, M. Kwakernaak, and J. Abeles, "Highly linear and efficient phase modulators based on GaInAsP-InP three-step quantum wells," Appl. Phys. Lett. **86** (3),p. 031103 (2005).

[6] C. Thirstrup, IEEE J. of Quantum Elect. **31**, 988 (1995).

[7] K. Ikossi , W.S. Rabinovich, D.S. Katzer, S.C. Binari, J. Mittereder, P.G. Goetz, "Multiple quantum well PIN optoelectronic devices and a method of restoring failed device characteristics," Microelectronics Reliability **42**, pp. 1021–1028, (2002).

[8] S. Griggs, M. Mark, B. Feldman, " Dynamic Optical Tags," Battlespace Digitization and Network-Centric Systems IV, edited by Raja Suresh, Proc. of SPIE Vol. 5441, pp. 151-160 (2004).